Intercluster charge ordering in monoclinic and triclinic Ba-Mo-based hollandite phases

Eslam M. Elbakry, [a] and Jared M. Allred * [a]

[a]Department of Chemistry and Biochemistry, The University of Alabama, Tuscaloosa, Alabama 35487, United States

*Email: jmallred@ua.edu

Supplementary information

Synthesis

Lowering the tube volume tended to enhance **TRI** phase yields, while increased volumes resulted in mixtures of **TRI** and **TET** phases, as shown in Figure (S2). This suggests that $BaCO_3$ decomposition has an activity or effective partial pressure of carbon dioxide that somehow favors the formation of the **TRI** hollandite phase. Since copper tubes showed no evidence of being pressurized after reaction, other possibilities were investigated. The reaction product showed no weight loss upon heating up to 800 °C under TGA (Figure S3), suggesting that CO_2 is not trapped in hollandite channels as it is in some cases.[30, 31]

It is plausible that CO_2 serves as an oxidizing agent, since thermodynamics favors its reaction with Mo to produce MoO_2 and C under similar conditions. While this would explain the need for a slight excess of Mo for optimal phase purity, the inherent difficulty in identifying trace elemental carbon has so far precluded further validation.

Extra details about the TRI single crystal structure solutions

A pseudo-merohedral twin law was included in the shelx refinement that exchanges the triclinic **b** and **c** axes. These axes correspond to the parent tetragonal phase **a** and **b** axes and they are only slightly distorted away from equivalence in the triclinic form. This was accomplished using the matrix TWIN matrix: [-1 0 0; 0 0 1; 0 1 0]. Though the refined phase fraction of the twin is less than 0.005, it was nonetheless statistically significant.

Extra details about the MON single crystal structure solutions

A pseudo-merohedral twin law was included in the shelx refinement that exchanges the monoclinic **a** and **c** axes. These axes correspond to the parent tetragonal phase **a** and **b** axes and they are only slightly distorted away from equivalence in the monoclinic form. This was accomplished using the matrix TWIN matrix: [0 0 1; 0 1 0; -1 0 0]. Though the refined phase fraction of the twin is less than 0.005, it was nonetheless statistically significant.

The independent refinement of thermal parameters of the four channel cation sites did not fully converge, so models that constrained similar channel sites to have equivalent ADP parameters were tested.

Confining thermal parameters of Ba1A with Ba1B, and Ba2A with Ba2B yielded wR_2 of 0.0654, while restricting ADP of Ba1A to Ba2A, and Ba1B to Ba2B gave wR2 of 0.0651, and thus the latter model was adopted. These parameters were also most similar in the freely refined model. In other words, structurally similar sites have similar U_{ij} values, as expected. Attempts were made to model the various Ba/Na sites as purely Ba or purely Na sites while still maintaining the same overall stoichiometry. Generally treating any site as purely Na breaks the model, while treating any site or group of sites as purely Ba merely increases the Na occupancy of the other sites while having a nearly insignificant effect on the R factors and total *A*-site occupancy. For this reason, the uniform occupancy model described in detail above is the preferred one that is reported in Table (3).

The disorder is reminiscent of the sort of phase shift scene in the modulated tetragonal structure $Ba_{8/7}Mo_8O_{16}$,[14] which exhibits local Mo_3 trimers, which tend to occur wherever two A-site cages are occupied. This implies that a more complex local bonding environment may be present than is seen in the average structure.

Secondly, the channel contains a continuum of residual electron density in the channels away from the main 4 Ba/Na sites, which we attribute to a result of aperiodic local structure distortions of the same type mentioned above. However, the residual density peak around the cage edge at 8.16 $e^-/Å^3$. Any extra partial occupancy site tends to refine toward that position, which also happens to be the location of the Na site in the original Lii model. Including the fifth site, labeled as Ba3/Na3 in Table (S3), reduces the wR2 from 0.0634 to 0.0476 with a maximum residual peak of 4.62 $e^-/Å^3$.

We could not justify assigning either purely Na or mixed Ba/Na to this site because it is essentially square planar with a four oxygen contacts equal to 2.20 Å. This would require a large displacement disorder in the local O sites that is contraindicated by the measured intensities. Even interpreting the extra site as a split site off the center produces unphysically short contacts between either Na and O or Ba and O. Also, constrained split-site models in this locale were generally unstable to refinement.

We interpret the location of the extra electron density around the cage edge as an artifact resulting from local structural modulation. It should be treated as part of the total electron density of the cage, and thus contribute to the stoichiometry, but it should not be treated as a minority site in terms of local environment. Diffuse scattering measurements are required to determine the actual local structure correlations.

Supporting Figures

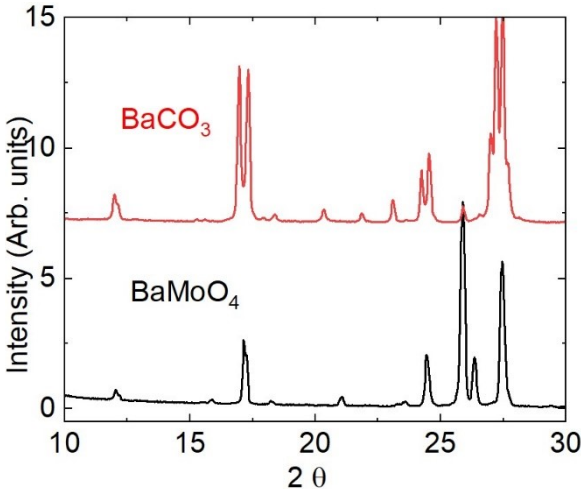

Figure (S1): Triclinic phase prepared in different Ba sources $BaCO_3$ (top, red) and $BaMoO_4$ (bottom, black). The $BaMoO_4$ is a mixture of tetragonal and triclinic polymorphs, which is distinguishable in the peak shoulders.

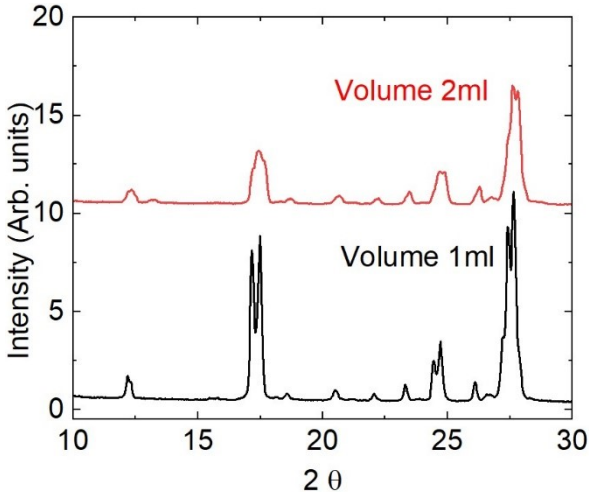

Figure (S2): Triclinic phase prepared in copper tubes of volumes 1 ml and 2 ml. The tetragonal polymorph is present in the 2 mL sample.

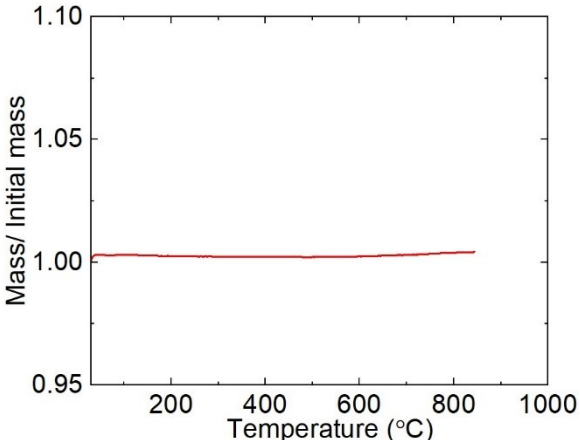

Figure (S3): Thermogravimetric analysis of the triclinic phase, **TRI**. One hypothetical CO_2 molecule per channel vacancy would contribute approximately 1% of the total mass of the compound.

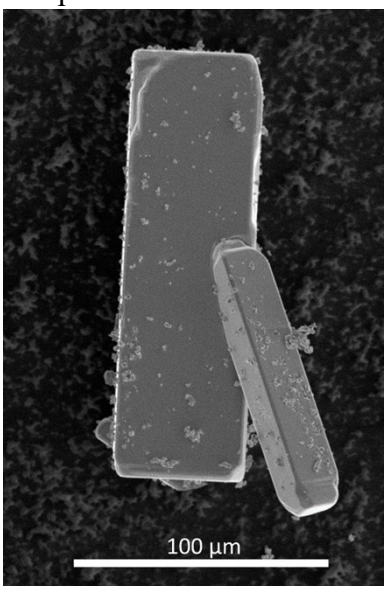

Figure (S4): SEM images of the tetragonal phase, **TET**, obtained by quenching.

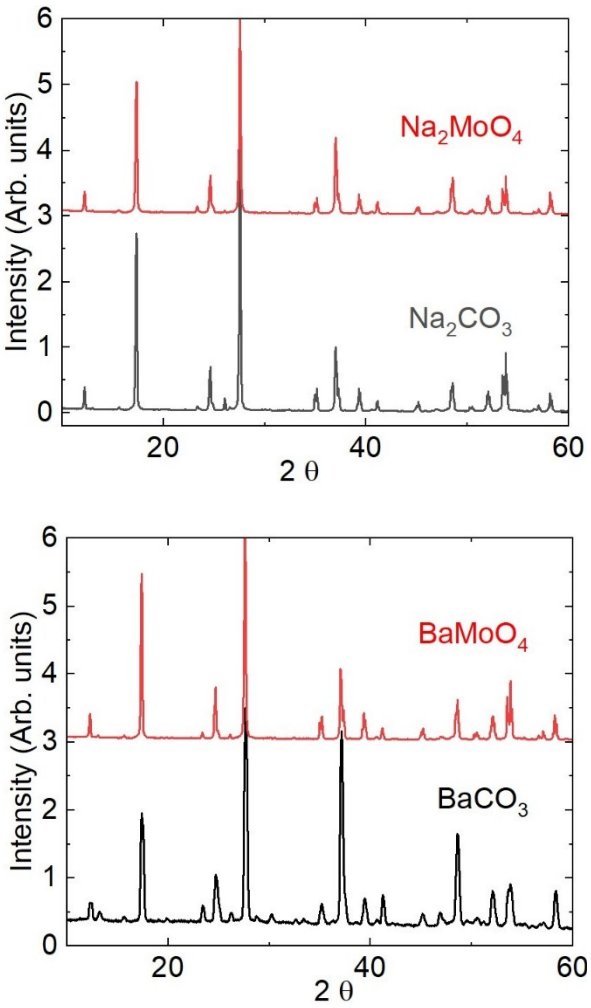

Figure (S5): PXRD patterns for **MON** phase obtained by different precursor compounds.

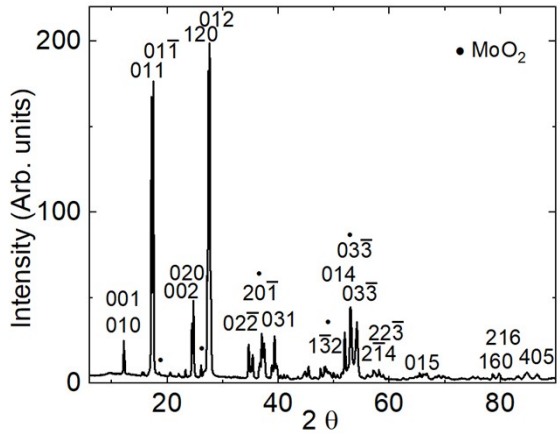

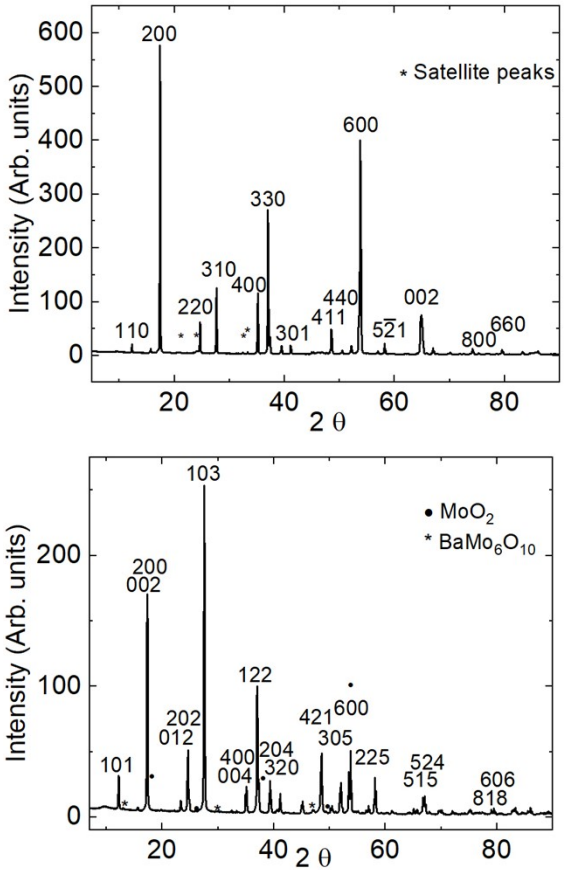

Figure (S6): PXRD pattern of **TRI**, **TET** and **MON** phases, from top to bottom, respectively.

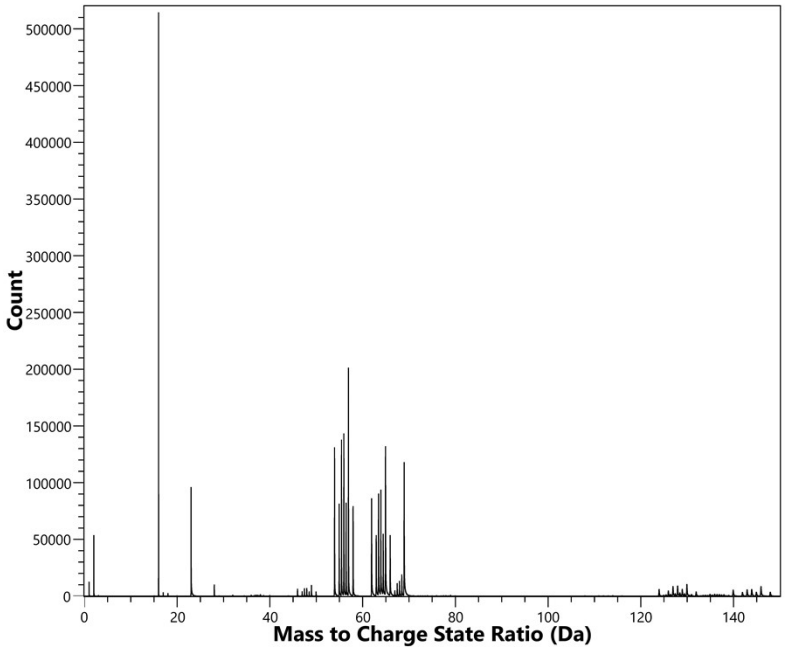

Figure (S7): Total mass spectrum of the MON phase.

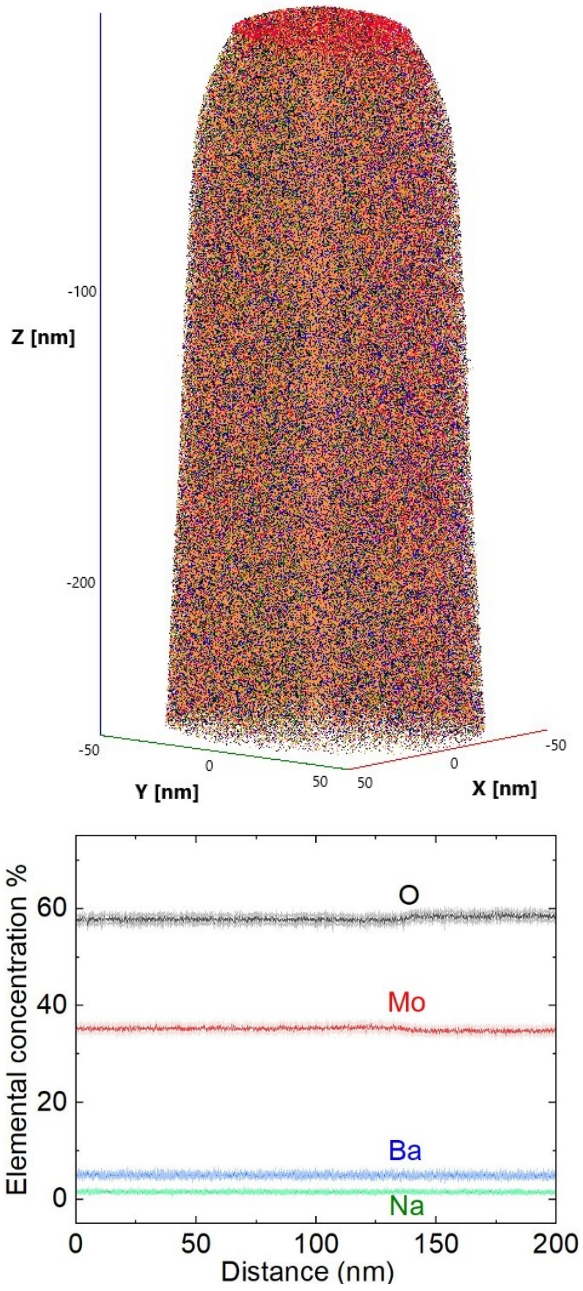

Figure (S8): Top: 3D reconstruction of a needle-shaped sample taken from a monoclinic crystal. Red, orange, blue, green, and black dots stand for Mo, molybdenum oxides ionic clusters, oxygen, sodium, and barium elements. Bottom: 1D concentrations of Na, Ba, and Mo normal to the c-axis. The small kink around 150 nm is a common effect that is attributed to surface oxidation during specimen fabrication.

Supplementary Tables

Table (S1): Unit cell dimensions of the newly synthesized triclinic compound, **TRI**, and the previously reported $Ba_{1.13}Mo_8O_{16}$ phase. Unit cell of **TRI** has been transformed to match the prior setting for comparison.

	$Ba_{1.12}Mo_8O_{16}$ (**TRI**, present work)	$Ba_{1.13}Mo_8O_{16}$ (Torardi and McCarley)[1]
a	7.31811(17) Å	7.311(1) Å
b	7.45804(14) Å	7.453(1) Å
c	5.73179(12) Å	5.726(1) Å
α	101.5137(17) °	101.49(2) °
β	99.5523(18) °	99.60(2) °
γ	89.2492(17) °	89.31(2) °
V	302.224(11) Å^3	301.40(7) Å^3

Table (S2): Unit cell dimensions of the newly synthesized monoclinic compound, and the previously reported $Na_{0.35}BaMo_8O_{16}$ phase. Note that the Lii cell has been transformed to match the setting used in our work.

	$Na_{1/3}BaMo_8O_{16}$ (**MON**, present work)	$Na_{0.35}BaMo_8O_{16}$ (Lii)[2]
a	10.22775(19) Å	10.231(3) Å
b	5.73224(12) Å	5.732(1) Å
c	10.2849(2) Å	10.289(2) Å
β	90.2821(18)°	90.28(2)°
V	602.98(2) Å^3	603.4(2) Å^3

Table (S3): Occupancies of the $Na_{0.33}BaMo_8O_{16}$ phase (**MON**) from a model that includes the residual electron density at the cage edge. Both Ba and Na values are derived from the same refined parameter per site.

Site label	Ba occ.	Na occ.	Total
1A	0.214(10)	0.069(3)	0.283(13)
1B	0.314(10)	0.102(3)	0.416(13)
2A	0.237(8)	0.077(2)	0.314(10)
2B	0.182(7)	0.059(2)	0.241(9)
3	0.0585(17)	0.0190(5)	0.0775(20)
Total	**1.006(18)**	**0.326(5)**	**1.332(21)**

References

(1) Torardi, C.; McCarley, R. Some reduced ternary and quaternary oxides of molybdenum. A family of compounds with strong metal-metal bonds. *Journal of Solid State Chemistry* **1981**, *37* (3), 393-397.

(2) Lii, K.-H. *Synthesis and characterization of some reduced ternary and quaternary molybdenum oxide phases with strong metal-metal bonds*; Iowa State University, 1985.